RSC Advances

PAPER

View Article Online
View Journal | View Issue

Cite this: *RSC Adv.*, 2017, **7**, 37000

A sulfonated polymer membrane with Ag-based graft: morphology, characterization, antimicrobial activity and interception ability

Qi He, Zipei Zhu, Hao Dong and Kaijun Xiao*

Ag-based nano-graft is a common approach used to impart broad-spectrum antimicrobial activity to a polymer membrane. The primary problem with this approach is low compatibility between the grafted particles and the polymer main-body, followed by its low anti-adhesion for undesired membrane fouling. To overcome these problems, this study functionalized polyethersulfone (PES) materials by a sulfonation process to form the membrane backbone. FTIR, thermogravimetry (TG) and contact angle (CA) analysis showed that sulfonate treatment improved hydrophilicity and surface activity. Accordingly, the Ag-based nano-grafts were embedded on the membrane by immersing into a Ag^+ solution and then reducing. The resulting membrane was characterized by a series of assays. SEM and AFM scans were used to examine the membrane surface for Ag nanoparticles (AgNPs) distribution. XRD and XPS analysis determined the AgNPs state. A concentration assay revealed that the Ag release from the membrane was maintained within the safety range during the filtration process. An antimicrobial ring test showed the antimicrobial activities of the membrane for different microbial strains. BET analysis and the water-absorption test analyzed the porosity properties of the membrane. The filtration performance assay proved that the membrane had remarkable interception ability for various solutes. Consequently, it showed that the prepared SPES-AgNPs membrane will have a promising application as an antimicrobial filtration membrane for water treatment.

Received 21st April 2017
Accepted 14th July 2017

DOI: 10.1039/c7ra04488g

rsc.li/rsc-advances

1. Introduction

Membrane filtration is a promising approach to purify wastewater. It has remarkable advantages, such as high energy-efficiency, high selectivity, high economic benefit and low pollution.[1] In recent years, with increasing demand for eco-friendly wastewater treatment technology, this approach has attracted more and more attention from both researchers and merchants.[2]

During the filtration process, biofouling is the most undesired problem. It can greatly impact membrane performance and is manifested by declining flux, increased energy cost and shortened lifetime.[3,4] Due to the special attached structure on microorganism cells, biofouling can hardly be cleaned.[5,6] Even worse, because of the microorganisms' self-replicating nature, biofouling will be enhanced geometrically during membrane use.[7]

The available strategies to solve this problem are mainly "anti-adhesion" or "antimicrobial".[8] On one hand, hydrophilic surfaces are much less likely to attach to bacteria, but most industrial polymeric membrane materials are hydrophobic.[9] Therefore, an effective anti-adhesion approach is to improve hydrophilicity of the polymer materials. On the other hand, a common approach for the "antimicrobial" strategy is to directly incorporate some biocides into the membrane.[10] A suitable antimicrobial compound is needed to balance antimicrobial activity and toxicity towards humans. Thus, AgNPs are of special interest as an antimicrobial additive.[11,12] Moreover, due to the advantages of easy handling, high solubility in organic solvents and outstanding chemical resistance, PES is considered as a hopeful material to form the membrane backbone.[13] Reportedly, the recent PES-Ag based products still have several defects including low hydrophilicity, low graft amount, high Ag release and short-lived antimicrobial activity.[14,15] Therefore, to solve these problems, this study initiates the introduction of $-SO_3H$ into the PES backbone. As a result, the prepared SPES-AgNPs membrane exhibits outstanding hydrophilicity and antimicrobial activities to reduce membrane fouling. It also shows some improvements in porosities and the ions' interception ability.

2. Experimental

2.1. Materials

PES (RADEL, A-300) was obtained from Amoco Chemicals, US. H_2SO_4 (98 wt%) and *N*,*N*-dimethylformamide (DMF) were

School of Food Science and Engineering, South China University of Technology, Guangzhou City, Guangdong Province, China, 510640. E-mail: fekjxiao@scut.edu.cn; Tel: +86 20 87113843

obtained from Donghong Chemical Plant, China. $AgNO_3$ (analytical grade) was obtained from National Pharmaceutical Group, China. Microbiology agars were obtained from Huankai Microbe Company, China. *Escherichia coli*, *Pseudomonas aeruginosa* and *Staphylococcus aureus* strains were obtained from Guangdong Province Bacteria Collection Center, China. Chemicals in this study were used without further purification.

2.2. PES sulfonation and characterization

The sulfonation process was performed in a professional laboratory with the necessary safety precautions. PES was dried at 120 °C overnight and sulfated by immersing into H_2SO_4 (98 wt%) with magnetic stirring at 60 °C (10 g SPES per 200 mL H_2SO_4).[16] After a period of reaction, the resulting mixture was injected slowly into ice water. The precipitate of raw SPES was obtained, thoroughly washed using deionized water until the pH approached 7, and dried under vacuum at 60 °C overnight.[16]

The ion exchange capacity (IEC) of the prepared SPES material was determined through the H^+ release amount. SPES material was minced into pieces with a size of several millimeters. The minced material was suspended in 2 M of NaCl solution (0.5 g SPES per 50 mL NaCl) for 24 h and titrated using a NaOH solution (0.1 M) with phenolphthalein as the indicator. The IEC was calculated by eqn (1):[17]

$$\text{IEC (mequiv./g)} = \frac{V_{\text{NaOH}} - V_{\text{NaCl}}}{1000 W_{\text{dry}}} \quad (1)$$

where V_{NaOH} and V_{NaCl} are the volume of used NaOH and NaCl, respectively; W_{dry} is the weight of dry PES.

Accordingly, the degree of sulfonation (DS) of the prepared SPES material was determined by eqn (2):[17]

$$\text{DS} = \frac{M_0 \text{IEC}}{1000 - M_{\text{SO}_3\text{Na}} \text{IEC}} \quad (2)$$

where M_0 (232 g mol^{-1}) and $M_{\text{SO}_3\text{Na}}$ (103 g mol^{-1}) were the molar masses of the initial polymer and the $-SO_3Na$ group, respectively.

Fourier transform infrared (FTIR) spectra of the prepared SPES material were investigated using a FTIR analyzer (Vector 33, Bruker Company, Germany); the analysis was carried out in the wavelength range 600–4000 cm.

The thermogravimetric (TG) properties of the prepared SPES material were determined using a TG analyzer (TA Q500, TA Company, US). The temperature range was controlled as 100–700 °C.

The hydrophilicity of the prepared SPES material was estimated using a contact angle (CA) goniometer (OCA15, Dataphysics Company, Germany).[18] Three repeats were performed for each membrane.

2.3. Preparation of membranes

The membrane-casting solution was prepared by dissolving the SPES material into DMF. Minced SPES (~15 wt%) was added into the solvent slowly, stirred at 60 °C until complete dissolution, and centrifuged at 4000 rpm for 3 min to eliminate foam. Then, the resulting solution was casted (~40 μm of thickness) on a clear glass plate using a casting knife in a stable environment (~21 °C, ~75% relative humidity). The casted glass plate was immersed into a water bath at ~21 °C for 24 h to form a membrane. The resulting membrane was washed using ethanol and air-dried at ~21 °C for 24 h.[12]

SPES-AgNPs membranes were prepared by loading AgNPs on the SPES membrane. The resulting membrane was immersed in 2.5 g L^{-1} of $AgNO_3$ aqueous solution for 2 h. The residual solvent on the surface was removed. Then, it was immersed in 0.25 mol L^{-1} of vitamin C aqueous solution for 15 min. After this, the membrane was washed using deionized water and air-dried at ~21 °C for 24 h. In addition, a PES-AgNPs membrane was prepared using a similar method as the control sample.[19]

2.4. Characterization of the membranes

2.4.1. Surface morphology observation. The microstructure of the prepared membranes was observed using a scanning electron microscope (SEM, Nova Nano 450, US) operating at 20 kV and 80 mA. In addition, the main elemental composition (C, S, O and Ag) on their surface was roughly determined using energy-dispersive X-ray spectrometry (EDS).[20]

The surface topologies of the prepared membranes were characterized using atomic force microscopy (AFM, Multimode 8, Bruker Company, Germany). In order to reduce errors, the roughness was reported as an average value.[21]

2.4.2. Ag release and antimicrobial activities. X-ray diffraction (XRD) patterns of the prepared membranes were recorded using a XRD instrument (D8 Advance, Bruker, Germany) equipped with Cu-Kα X-ray radiation.[22] It was conducted to investigate the presence of the silver element on the membranes. In addition, a further analysis was carried out using an X-ray photoelectron spectrophotometer (XPS, JPS-9000SX, JEOL, Japan) with a Mg-Kα-radiation source (1253.6 eV).[23]

Ag release was monitored by measuring its concentration in a filtration test. Each membrane (100 cm^2) was used in a water filtration process with a flux of ~100 L m^{-2} h^{-1} at room temperature (~20 °C). Every 2 h, a water sample was obtained from the permeate side and the Ag concentration in this sample was analyzed using an atomic absorption spectrometer (AAS, Z-2000, Hitachi, Japan).[23]

The antimicrobial activities of the prepared membranes were assessed using two Gram-negative bacteria (*E. coli* and *P. aeruginosa*) and a Gram-positive bacterium (*S. aureus*). Each membrane was cut as a small disk (1 cm of diameter) and placed on a nutrient agar that had been inoculated with different microbial strains. The resulting agars were incubated for 24 h at 37 °C. Then, the colonies obtained on the agar were counted. Three replicates were performed for each measurement.[24]

A further study was performed *via* bacterial suspensions. Some disks of each membrane (about 0.5 g) were immersed into 10 mL of different bacterial suspensions (108 CFU mL^{-1}) and cultured in a table concentrator with suitable shaking at 37 °C for 2 h. Then, the bacterial suspension was diluted into a suitable concentration with sterile water, inoculated on LB solid

medium, and cultured at 37 °C for 24 h. Three replicates were performed for each membrane. The antimicrobial rate was calculated by eqn (3):[25]

$$G = \frac{N_0 - N_m}{N_0} \quad (3)$$

where G is the antimicrobial rate; N_m and N_0 are the colony counts of the bacterial suspension with and without the membrane disks, respectively.

2.4.3. Porosity properties and filtration performance. Brunauer–Emmett–Teller (BET) porosity properties of the prepared membranes were measured by a nitrogen adsorber (JW-BK222, JWGB, China). The pore size distribution was calculated by the equipped analysis software using the density functional theory (DFT) method.[26]

The water-absorption porosities (ε) of the prepared membranes were investigated according to the method described by Basri *et al.*[27] A dry membrane was weighed and the weight was recorded as W_{dry}. Then, it was immersed in distilled water at ~21 °C and periodically re-weighed until its weight was constant (W_{wet}). The ε value was calculated by eqn (4):

$$\varepsilon = \frac{W_{wet} - W_{dry}}{\rho_w V} \quad (4)$$

where ρ_w was the density of pure water at room temperature and V was the volume of the membrane in the wet state.

The filtration performance of the prepared membranes was evaluated using a 1 g L^{-1} bovine serum albumin (BSA) solution (pH = 7.4) and 4 types of 2 w/v% aqueous solutions with inorganic matter (NaCl, Na_2SO_4, $MgCl_2$ and $MgSO_4$). The initial concentration and the concentration in the permeated liquid were recorded as c_0 and c, respectively, for the interception rate (IR) calculation. The concentrations of BSA were measured using an ultraviolet spectrophotometer (UV, D-8PC, Phelps Company, China) at 278 nm, while the concentrations of target salts were measured using AAS. The IR were calculated by eqn (5):[28]

$$IR = \frac{c_0 - c}{c_0} \times 100\% \quad (5)$$

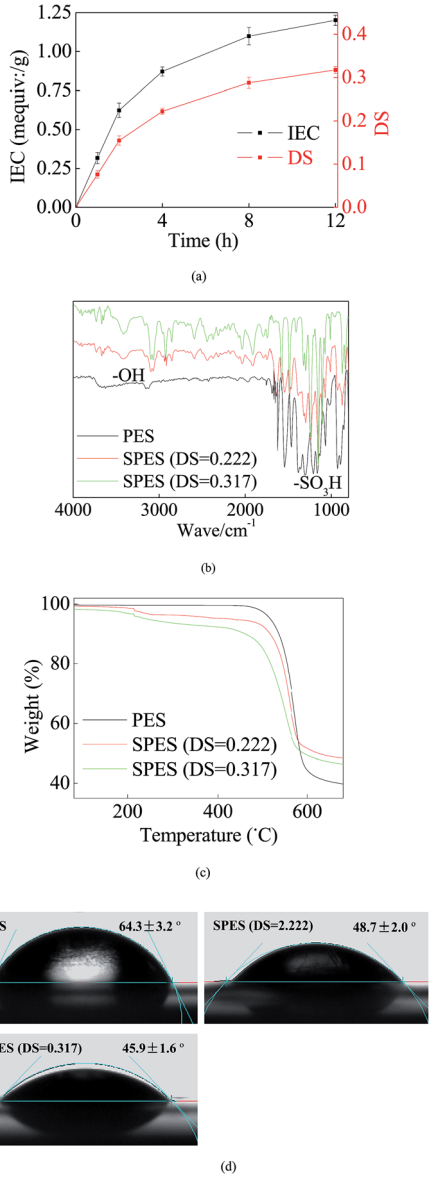

Fig. 1 PES sulfonation properties. (a) IEC and DS; (b) FTIR spectra; (c) TG and (d) CA.

3. Results

3.1. PES sulfonation and characterization

During SPES sulfonation, sulfuric acid groups (–SO_3H) were grafted into PES particles and could be considered as a replacement of the –H site.[29] Initially, a great number of sites were available for the graft of –SO_3H. Thus, the growth trend of both IEC and DS was rapid (Fig. 1a). With increasing reaction time, most of the accessible sites were occupied and it strongly repelled more –SO_3H groups; hence, the growth trends of IES and DS slowed down and tended to equilibrium gradually. Reasonably, a higher DS improves the performance of the SPES material, but it also indicates a geometric increase of the preparation time in the sulfonation process. Moreover, when the DS of SPES is higher than 0.4, SPES will be partly dissolved in water and it is bad for membrane preparation.[29] Thus, with a balance between the performance and the cost, the SPES material with a DS of 0.317 was selected as the membrane material in the next step.

Fig. 1b illustrates the FTIR results. Significant characteristic peaks of –SO_3H groups (~1100 cm^{-1}) were found in the curve of SPES. Another noteworthy characteristic peak was presented at ~3200 cm^{-1}. It represented the reflection of hydroxyl groups (–OH).[11] The presence of –OH was a sign of hydration. It further suggested the remarkable hydrophilicity of SPES.[11] Moreover, due to O particles having great electronegativity, the presence of –OH can establish strong links with the loading AgNPs.

The TG results are shown in Fig. 1c. When temperature was less than ~200 °C, no significant weight loss was found in each material. When the temperature was 200–450 °C, a slight weight loss was presented in the SPES material due to the decomposition of sulfonic acid groups.[30] When the temperature

increased to 450–600 °C, the PES chain that formed the membrane backbones broke down, and thus both PES and SPES experienced great weight loss (40–60%).

Higher hydrophilicity yielded better wettability that could suppress concentration polarization on the membrane surface. Consequently, it improved membrane resistance for pollution fouling.[31] As shown in Fig. 1d, the CA of the PES membrane was 64.3 ± 3.2°. Moreover, the presence of $-SO_3H$ enhanced the hydrophilicity of SPES. Thus, the CAs of the SPES membrane was less than 50%. Reportedly, the CAs of common commercial seawater reverse osmosis (RO) membranes were usually limited at the range of 25–60°.[32] In this study, the SPES membrane was within this range. This revealed that the prepared SPES membrane was suitable as a RO membrane for water treatment.

3.2. Micro-structure observation

Fig. 2 showed the surface structure of the prepared membrane. On surface of the SPES membrane, numerous fully developed voids were distributed. As a rough estimate, their scale was from tens to one hundred nanometers, indicating that the prepared SPES membrane might belong to an ultra-filtration (UF) membrane. On surface of the SPES-AgNPs membrane, AgNPs were fully dotted. Most of them were less than ~100 nm in diameter. When it comes to the PES-AgNPs membrane, much less AgNPs were distributed on the surface due to the low compatibility of PES materials. Such a difference can be quantized by EDS analysis for four elements (C, O, S and Ag). As shown in Fig. 2, the SPES-AgNPs membrane was detected to exhibit more than double the Ag content (21.9%) compared to PES-AgNPs membrane (8.4%).

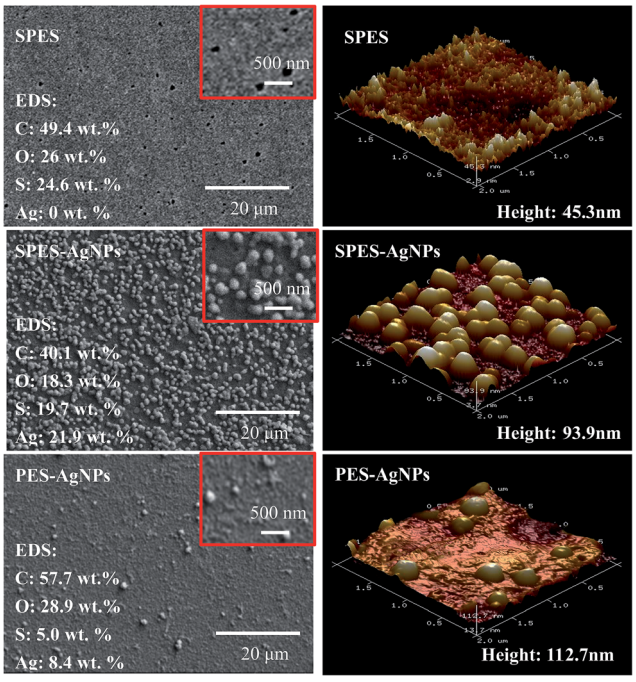

Fig. 2 SEM and AFM results of the SPES membrane; SPES-AgNPs membrane; and PES-AgNPs membrane.

The topology of the membrane surface was observed in the AFM results. Among them, the SPES membrane had a relatively smoother surface with a height of 45.3 nm. Moreover, because of the graft of AgNPs on the surface, the height of the SPES-AgNPs and the PES-AgNPs membrane increased to ~100 nm.

3.3. Grafted Ag properties and antimicrobial activities

XRD analysis was conducted to describe the Ag loading state. As shown in Fig. 3a, pure SPES material was characterized as a typical non-crystalline structure with a series of characteristic peaks at 2θ values of 22–26°, while Ag was reflected at 4 typical diffraction peaks with 2θ values of 38.2°, 43.8°, 64.7° and 77.2°.[33] Both SPES-AgNPs and PES-AgNPs included significant characteristic peaks of the Ag element, while the reflection intensity of the PES-AgNPs membrane was weaker than that of SPES-AgNPs.

XPS results can also prove a similar conclusion. Reportedly, the Ag^0 element has two typical XPS peaks centered at binding energies (BE) 369.4 eV (Ag 3d5/2) and 375.8 eV (Ag 3d3/2).[34] As shown in Fig. 3b, corresponding peaks were found at the curve of both the SPES-AgNPs membrane (369.5 eV and 375.8 eV) and the PES-AgNPs membrane (369.1 eV and 375.3 eV). Similarly, the peak intensities of the SPES-AgNPs membrane were significantly stronger than the PES-AgNPs membrane.

In addition, Fig. 3c illustrated the possible formations for the interaction between SPES monomers and grafted AgNPs.[27] The Ag^0 atoms are prone to the loss of electrons and change into Ag^+, while the O atoms ($1s^2\ 2s^2\ 2p^4$) from the SPES material have 2 lone-pairs of electrons that can form a coordination bond with Ag^+. Moreover, with the attraction of the S^{5+} particle in the $-SO_3$ groups, the O atoms from the $-SO_3$ groups more easily attract Ag^+ and have stronger links compared to the phenyl oxygen in the main chain.[27] Thus, we can infer that the PES-AgNPs membrane more easily loses its grafted Ag^+ compared to the SPES-AgNPs membrane. This can be proven by the Ag release results, as shown in Fig. 3d. On both membranes, Ag release showed a gradual decrease, while the downward trend of the SPES-AgNPs membrane was much gentler compared to the PES-AgNPs. Another notable point is that the accumulation of Ag should balance the antimicrobial activity and toxicity towards humans. Based on the safety standards reported by the WHO for drinking water (100 μg L^{-1}),[35] the use of the SPES-AgNPs membrane can always remain in a safe range, while the PES-AgNPs membrane was beyond the limitation at the first time. Furthermore, when taking the total Ag content into consideration, the SPES-AgNPs membrane released only 3.35% of its total AgNPs in the first 24 hours, while PES-AgNPs only released 8.58%, indicating that the SPES-AgNPs membrane may have more than double the antimicrobial shelf life of the PES-AgNPs membrane. Fig. 3e described the inhibition zone results. The pure SPES membrane only slightly impacted the bacteria, because $-SO_3H$ is a strong oxidizing agent that can kill some microbes. In comparison, SPES-AgNPs and PES-AgNPs membranes showed significant antimicrobial activities. The AgNPs is believed to act as an outstanding antimicrobial agent.[36] Its ions diffused away from the membrane and killed

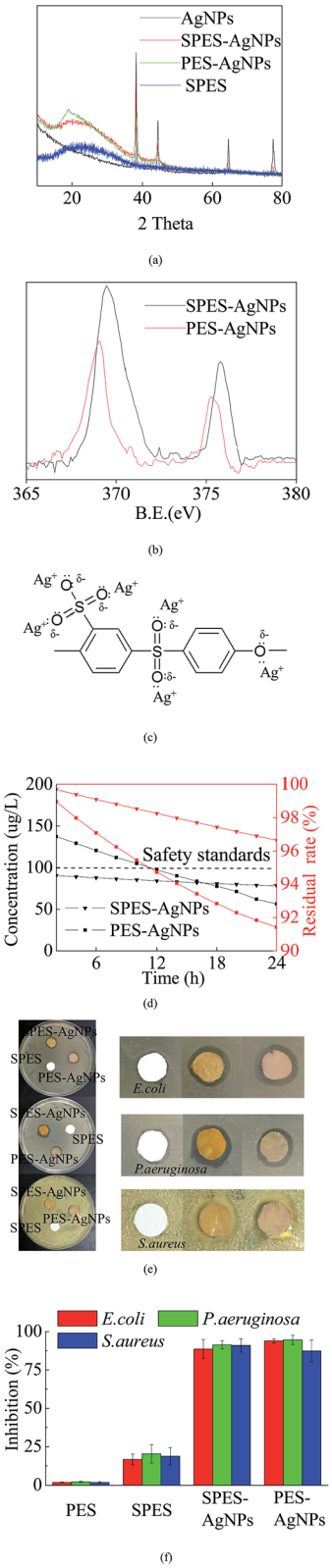

Fig. 3 The loading AgNPs properties (a) XRD results; (b) XPS results; (c) possible interactions (d) Ag release and antibacterial effects (e) inhibition zone; and (f) suspensions inhibition rate of the prepared membranes.

microbes in the area along the outer edge of the membrane disks, resulting in a wide inhibiting ring. Such antimicrobial activity was quantized by the results using suspensions (as Fig. 3f). The inhibition using the PES and the SPES membrane was less than 25%, while either the SPES-AgNPs or the PES-AgNPs membrane was more than 80%. When it comes to the difference from different microbial strains, the overall inhibition from strongest to weakest ranked as follows: *P. aeruginosa* > *S. aureus* > *E. coli*.

3.4. Porosity properties and filtration performance

Fig. 4a described the results of BET analysis. As is shown, each membrane had similar N_2 adsorption–desorption isotherms, characterized by an upward convex that matched the type I isotherm.[37] In addition, it could be found that the pore size distribution of the AgNPs grafted membrane was broader than that of the SPES membrane, which was caused by the graft of the AgNPs blocking the pores on the membrane surface.[38] The result was characterized by the differences in total pore volume, as detailed in Fig. 4b. Moreover, the results of the water-absorption porosity test showed a similar trend.

During the operating process of a membrane for water treatment, its performance is to a great extent determined by the selective interception capacity for given compounds of

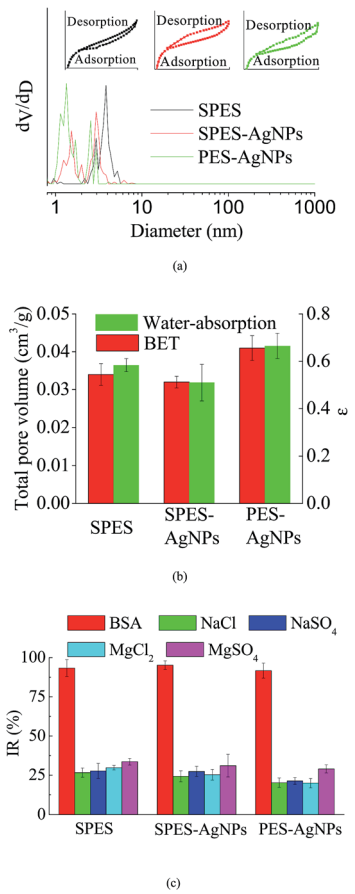

Fig. 4 (a) BET results; (b) porosity properties; and (c) interception capacity of the prepared membranes.

Table 1 Performance of different Ag-PES membranes

Membranes	Thickness (μm)	CA (°)	Flux (L m^{-2} h^{-1})	BSA rejection (%)	Porosity ε (%)	Mean pore size (nm)	Ref.
NanoAgZ-PES	—	52.6–71.5	82.1–110.6	96.1–98.5	—	—	8
PES	~100	59.85	—	—	0.038	10.30	12 and 27
PES/Ag	~100	50.97	—	—	0.038	3.74	
PES/PVP/Ag	~100	47.85	—	—	0.203	0.92	
PES/TAP/Ag	~100	42.06	—	—	0.104	1.45	
PES-Am-Ag	—	—	~120	~60	—	—	14
Bio-Ag^0/PES	~140	51.4–66.6	150–500	—	—	—	15
SPES-AgNPs	~40	~45	~100	95.2	0.509	~4	This work

organic substances or inorganic salts. Fig. 4c summarizes the performance of the prepared membranes for different substances during the filtration process. As is shown, different prepared membranes displayed remarkable interception capacity. Synthetically, the PES-AgNPs membrane showed the best interception capacity. This could be explained by the fact that the AgNPs blocked some voids that could be available for solute substances.

4. Discussion

In this study, the antimicrobial PES membrane was prepared with the introduction of $-SO_3H$ active groups on its surface. The main improvement was reflected in its hydrophilicity and compatibility. Compared to the traditional pure PES, its links with Ag were greatly strengthened. Thus, the Ag release and resulting antimicrobial activity was more stable and sustainable. An example was reported by Basri *et al.*[12] who prepared a PES-Ag membrane using polyvinylpyrolidone (PVP) as a dispersant. The defects were reflected in both hydrophilicity and Ag release. Their further study[27] explained that the problem was caused because of the low compatibility between Ag and the polymers. Another representative study was performed by Zhang *et al.*,[15] which aimed to embed bio-Ag^0 in PES membranes. The performance of this product was slightly improved, but the compatibility problem was unsolved (as Table 1).

Moreover, compared to some other studies using a complex additive or modification, our materials were relatively cheap and common, while the preparing process was simple and well developed. Huang *et al.*[8] prepared a nanoAgZ-PES membrane. The prepared membrane had a comparable flux, a similar antimicrobial activity for *E. coli* and *P. aeruginosa* and a slightly superior IR for BSA. However, this study used a rare material, nanoAgZ. Sawada *et al.*[14] added an extra acrylamide (CA) layer as the medium between the PES layer and grafted Ag. Its overall performance was slight weaker than our product. Furthermore, the introduction of the CA layer greatly complicated the preparation process, as well as reduced the reliability.

5. Conclusions

In this study, an antimicrobial membrane was prepared by grafting the AgNPs on the sulfonated membrane backbone. FTIR, thermogravimetry (TG) and contact angle (CA) analysis showed that sulfonate treatment improved the hydrophilicity and the surface activity of the membrane material. Thus, Ag nanoparticles (AgNPs) were grafted on the membrane more easily and stably. SEM and AFM scans illustrated that there were more AgNPs on the sulfonated membrane, while XRD and XPS analysis also determined that the sulfonated membrane had a stronger reflection of Ag. In addition, a concentration assay revealed that Ag release from the membrane was maintained with in the safety range during the filtration process, resulting in significant antimicrobial activity for different microbial strains. Moreover, the BET analysis and the water-absorption porosity test evaluated the porosity properties. A filtration performance assay proved that the membrane had remarkable interception ability for various common solutes.

Acknowledgements

The authors are grateful for the financial support by Guangzhou Science and Technology Program Key Projects (201508020086), the Science and Technology Equipment Mobilization Project of Guangdong Province (x2skB2160440) and the Applied Science and Technology Research and Development Special Project of Guangdong Province (2015B020230001).

References

1 H. M. Yeh, H. Y. Chen and K. T. Chen, *J. Membr. Sci.*, 2000, **168**, 121–133.
2 K. N. Bourgeous, J. L. Darby and G. Tchobanoglous, *Water Res.*, 2001, **35**, 77–90.
3 J. Lee and I. S. Kim, *Desalination*, 2011, **273**, 118–126.
4 J. S. Vrouwenvelder, M. C. M. van Loosdrecht and J. C. Kruithof, *Desalination*, 2011, **265**, 206–212.
5 M. Herzberg and M. Elimelech, *J. Membr. Sci.*, 2007, **295**, 11–20.
6 S. Silver, *FEMS Microbiol. Rev.*, 2003, **27**, 341–353.
7 P. Landini, D. Antoniani, J. G. Burgess and R. Nijland, *Appl. Microbiol. Biotechnol.*, 2010, **86**, 813–823.
8 J. Huang, G. Arthanareeswaran and K. S. Zhang, *Desalination*, 2012, **285**, 100–107.
9 L. F. Hancock, S. M. Fagan and M. S. Ziolo, *Biomaterials*, 2000, **21**, 725–733.

10 Q. Li, S. Mahendra, D. Y. Lyon, L. Brunet, M. V. Liga, D. Li and P. J. J. Alvarez, *Water Res.*, 2008, **42**, 4591–4602.
11 F. C. Tenover, *Am. J. Med.*, 2006, **119**, 3–10.
12 H. Basri, A. F. Ismail, M. Aziz, K. Nagai, T. Matsuura, M. S. Abdullah and B. C. Ng, *Desalination*, 2010, **261**, 264–271.
13 H. Susanto and M. Ulbricht, *J. Membr. Sci.*, 2009, **327**, 125–135.
14 I. Sawada, R. Fachrul, T. Ito, Y. Ohmukai, T. Maruyama and H. Matsuyama, *J. Membr. Sci.*, 2012, **387–388**, 1–6.
15 M. Y. Zhang, K. S. Zhang, B. D. Gusseme and W. Verstraete, Biogenic silver nanoparticles (bio-Ag^0) decrease biofouling of bio-Ag^0/PES nanocomposite membranes, *Water Res.*, 2012, **46**, 2077–2087.
16 A. Rahimpour, M. Jahanshahi, B. Rajaeian and M. Rahimnejad, *Desalination*, 2011, **278**, 343–353.
17 A. Rahimpour, S. S. Madaeni, S. Ghorbani, A. Shockravi and Y. Mansourpanah, *Appl. Surf. Sci.*, 2010, **256**, 1825–1831.
18 C. Fang, Y. Jing and Z. X. Lin, *Int. J. Adhes. Adhes.*, 2017, **73**, 1–7.
19 A. Rahimpour and S. S. Madaeni, *J. Membr. Sci.*, 2010, **360**, 371–379.
20 C. Nadejde, M. Neamtu, R. J. Schneider, V. D. Hodoroaba, G. Ababei and U. Panne, *Appl. Surf. Sci.*, 2015, **352**, 42–48.
21 E. Yuliwati, A. F. Ismail, T. Matsuura, M. A. Kassim and M. S. Abdullah, *Desalination*, 2011, **283**, 206–213.
22 S. B. Hammouda, N. Adhoum and L. Monser, *J. Hazard. Mater.*, 2015, **301**, 350–361.
23 Q. He, J. L. Dai, L. Zhu, S. F. Li, K. J. Xiao and Y. R. Yin, *Sci. Adv. Mater.*, 2016, **8**, 1878–1886.
24 Q. He and K. J. Xiao, *Food Control*, 2016, **69**, 339–345.
25 B. P. Tripathi, N. C. Dubey, S. Choudhury, S. Choudhury, F. Simon and M. Stamm, *J. Mater. Chem. B*, 2013, **1**, 3397–3409.
26 Q. He, J. L. Dai, L. Zhu, K. J. Xiao and Y. R. Yin, *J. Alloys Compd.*, 2016, **687**, 326–333.
27 H. Basri, A. F. Ismail and M. Aziz, *Desalination*, 2012, **287**, 71–77.
28 R. Li, F. F. Liu and J. F. Deng, *Adv. Mater. Res.*, 2013, **800**, 606–609.
29 C. Manea and M. Mulder, *J. Membr. Sci.*, 2002, **206**, 443–453.
30 A. Chandra, *Polym. Bull.*, 2016, **73**, 2707–2718.
31 S. Kim and E. M. V. Hoek, *Desalination*, 2005, **186**, 111–128.
32 O. Akin and F. Temelli, *Desalination*, 2011, **278**, 387–396.
33 P. F. Andrade, A. F. de Faria, S. R. Oliveira, M. A. Arruda and M. C. Gonçalves, *Water Res.*, 2015, **81**, 333–342.
34 H. Kong and J. Jang, *Chem. Commun.*, 2006, 3010–3012.
35 M. Zhang, R. W. Field and K. Zhang, *J. Membr. Sci.*, 2014, **471**, 274–284.
36 K. Chaloupka, Y. Malam and A. M. Seifalian, *Trends Biotechnol.*, 2010, **28**, 580–588.
37 Q. He, Y. Shen, K. J. Xiao, J. Y. Xi and X. P. Qiu, *Int. J. Hydrogen Energy*, 2016, **41**, 20709–20719.
38 K. S. W. Sing, *Pure Appl. Chem.*, 1982, **54**, 2201–2218.